Facile Reversible Metalation in an Agostic Complex and Hydrogenolysis of a Metal Aryl Complex via a Dihydrogen Complex

Ana C. Albéniz,* Gayle Schulte, and Robert H. Crabtree

Sterling Chemistry Laboratory, Yale University, 225 Prospect Street, New Haven, Connecticut 06511

Received August 19, 1991

2,6-Diarylpyridines, 2,6-$(p\text{-}C_6H_4R')_2C_5H_3N$ (diarpyH$_2$: R′ = H, diphpyH$_2$; R′ = CH_3, ditolpyH$_2$) react with $[(COD)Ir(PR_3)_2]X$ (1; PR_3 = PPh_3, $P(p\text{-}C_6H_4CH_3)_3$, $P(p\text{-}C_6H_4F)_3$, PPh_2Me, P-*n*-Bu_3; X = SbF_6^-, BF_4^-) under H_2 to give complexes with the stoichiometry $[Ir(diarpyH)H(PR_3)_2]X$ (**2a–f**). The X-ray crystal structure for $[Ir(diphpyH)H\{P(p\text{-}C_6H_4CH_3)_3\}_2]SbF_6$ (**2b**) shows that one phenyl group of the diphpyH is orthometalated and the other is bound to the Ir via an agostic C–H bond. The Ir···C distance of the Ir···H–C group is 2.69 Å, indicating a moderately strong agostic interaction. **2b** crystallizes in the triclinic system, space group $P\bar{1}$, with a = 11.072 (2) Å, b = 14.450 (2) Å, c = 17.227 (2) Å, α = 92.76 (1)°, β = 105.04 (1)°, γ = 95.00 (1)°, and Z = 2. The complexes **2a–f** show dynamic behavior in solution, consistent with rapid oxidative addition of the agostic C–H bond together with reductive elimination of the aryl hydride. Ligands like CO or CH_3CN displace the agostic C–H in **2a** to give $[Ir(diphpyH)HL(PPh_3)_2]SbF_6$ (L = CO, **3**; CH_3CN, **4**). H_2 reacts with **2d** (PR_3 = PPh_2Me) and **2e** (PR_3 = P-*n*-Bu_3) in the same way to give the dihydrogen complexes $[Ir(diphpyH)H(\eta^2\text{-}H_2)(PR_3)_2]SbF_6$ (**5d,e**). Reversible Ir–Ar hydrogenolysis occurs with H_2 for **2a–c** and **2f**; an equilibrium between the dihydrogen complex **5** and the hydrogenolysis product $[Ir(diphpyH_2)(H)_2(PR_3)_2]SbF_6$ (**6**) is observed at low temperatures. For a given diarpyH ligand, less basic phosphines favor the hydrogenolysis product. Longer treatment of **2a** with H_2 leads to complete displacement of the diarpyH$_2$ ligand from the metal.

Introduction

One of the most interesting recent discoveries in coordination chemistry is the ability of a variety of X–H bonds to bind to unsaturated metal fragments. Perhaps the most important cases involve the C–H[1,2] and H–H bonds.[3] Such binding is believed to be favored when the M(d_π) orbitals have relatively low basicity and so are unable to donate sufficient electron density to the X–H σ^* orbital to break the X–H bond and form the oxidative-addition product X–M–H (eq 1). Binding as X–H···M should allow the

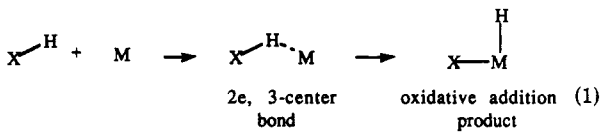

(1)

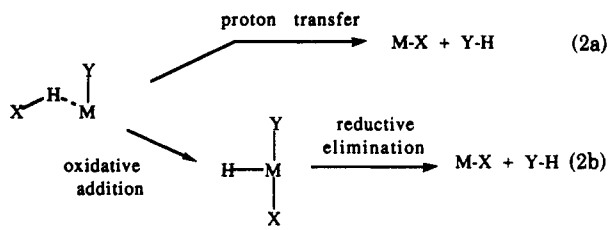

X–H bond to be activated without requiring oxidative addition. Now that the existence of these X–H···M species is well established, there is growing interest in their reactions. It has generally been assumed[1a,g] that such species are intermediates in oxidative addition, but evidence for this view has been sparse.

A few dihydrogen complexes[3] of the type $L_nM(\eta^2\text{-}H_2)$ have been shown[4] to be in equilibrium with the corresponding dihydrides $L_nM(H)_2$. The activation energy for the exchange is usually ca. 10 kcal/mol. This may mean that H_2 complexes are generally on the pathway for oxidative addition of H_2.

While simple C–H oxidative-addition reactions, such as orthometalation,[5] are now common, few clearly involve an agostic species or are reversible under mild conditions.[6] In only one example of reversible orthometalation can the agostic species be identified.[7] In a number of systems[8,9] catalytic deuteration of the ortho positions of PAr_3 ligands implies that reversible orthometalation is taking place, but intermediates are not seen. In this paper we have been able to study this process directly by looking at a degenerate rearrangement between C–H···M–C and C–M···H–C in an iridium complex.

(1) (a) Brookhart, M.; Green, M. L. H. *J. Organomet. Chem.* **1983**, *250*, 395. (b) Crabtree, R. H.; Hamilton, D. G. *Adv. Organomet. Chem.* **1988**, *28*, 299. (c) Brookhart, M.; Green, M. L. H.; Wong, L. *Prog. Inorg. Chem.* **1988**, *36*, 1. (d) Cotton, F. A.; Luck, R. L. *Inorg. Chem.* **1989**, *28*, 3210. (e) Jordan, R. F.; Bradley, P. K.; Baenziger, N. C.; LaPointe, R. E. *J. Am. Chem. Soc.* **1990**, *112*, 1289. (f) Seyler, J. W.; Fanwick, P. E.; Leidner, C. R. *Inorg. Chem.* **1990**, *29*, 2121. (g) Cotton, F. A.; Stanislowski, J. *J. Am. Chem. Soc.* **1774**, *96*, 5074.

(2) Crabtree, R. H. *Chem. Rev.* **1985**, *85*, 245.

(3) Kubas, G. J. *Acc. Chem. Res.* **1988**, *21*, 120.

(4) (a) Kubas, G. J.; Unkefer, C. J.; Swanson, B. I.; Fukushima, E. F. *J. Am. Chem. Soc.* **1986**, *108*, 7000. (b) Khalsa, G. R. K.; Kubas, G. J.; Unkefer, C. J.; Van Der Sluys, L. S.; Kubat-Martin, K. A. *J. Am. Chem. Soc.* **1990**, *112*, 3855. (c) Luo, X.-L.; Crabtree, R. H. *J. Am. Chem. Soc.* **1990**, *112*, 6912. (d) Conroy-Lewis, F. M.; Simpson, S. J. *J. Chem. Soc., Chem. Commun.* **1987**, 1675. (e) Chinn, M. S.; Heinekey, D. M. *J. Am. Chem. Soc.* **1990**, *112*, 5166. (f) Cappellani, E. P.; Maltby, P. A.; Morris, R. H.; Schweitzer, C. T.; Steele, M. R. *Inorg. Chem.* **1989**, *28*, 4437. (g) Arliguie, T.; Chaudret, B. J. *J. Chem. Soc., Chem. Commun.* **1989**, 155.

(5) (a) Parshall, G. W. *Acc. Chem. Res.* **1970**, 139. (b) Bruce, M. I. *Angew. Chem., Int. Ed. Engl.* **1977**, *16*, 73. (c) Omae, I. *Coord. Chem. Rev.* **1980**, *32*, 235.

(6) (a) Chatt, J.; Davidson, J. M. *J. Chem. Soc.* **1965**, 843. (b) Burk, M. J.; Crabtree, R. H. *J. Am. Chem. Soc.* **1987**, *109*, 8025. (c) Baker, M. W.; Field, L. D. *Organometallics* **1986**, *5*, 821. (d) Thomson, M. E.; Baxter, S. M.; Bulls, A. R.; Burger, B. J.; Nolan, M. C.; Santarsiero, B. D.; Schaefer, W. P.; Bercaw, J. E. *J. Am. Chem. Soc.* **1987**, *109*, 203.

(7) Cree-Uchiyama, M.; Shapley, J. R.; St. George, G. M. *J. Am. Chem. Soc.* **1986**, *108*, 1316.

(8) Crabtree, R. H.; Holt, E. M.; Lavin, M.; Morehouse, S. M. *Inorg. Chem.* **1985**, *24*, 1986.

(9) (a) Parshall, G. W.; Knoth, W. H.; Schunn, R. A. *J. Am. Chem. Soc.* **1969**, *91*, 4990. (b) Kiffen, A. A.; Masters, C.; Rayman, L. *J. Chem. Soc., Dalton Trans.* **1975**, 853.

0276-7333/92/2311-0242$03.00/0

Depletion of the electron density in the X–H bond[1,3] seems to take place on binding as X–H···M, and this can lead to the system acting as a proton donor.[1-3] If a basic M–Y bond is cis to the X–H···M system, this proton might be transferred to the M–Y bond and lead to the liberation of H–Y (eq 2a). In the case of H_2, this is the hydrogenolysis reaction. It remains to be established if H_2 complexes are important in such reactions. One difficulty is that a plausible mechanism can be envisaged involving reductive elimination of H–Y from the oxidative-addition product (eq 2b), and it will therefore be difficult to exclude the intervention of this intermediate in the overall reaction. The hydrogenolysis of M–C bonds is believed to be important in certain hydrogenation catalysts[2,10] and is an example of an important class of reaction, the σ-bond metathesis.[6d,11] In this paper, we study a reversible hydrogenolysis in the same Ir system.

In prior related work,[8] reaction of $[(COD)Ir(PR_3)_2]X$ with H_2 and 8-methylquinoline has been shown to give an agostic system, involving the quinoline methyl group. In contrast, 7,8-benzoquinoline undergoes cyclometalation of its aromatic C–H bond, and the product reacts with H_2 to give an η^2-H_2 complex[12] (eq 3).

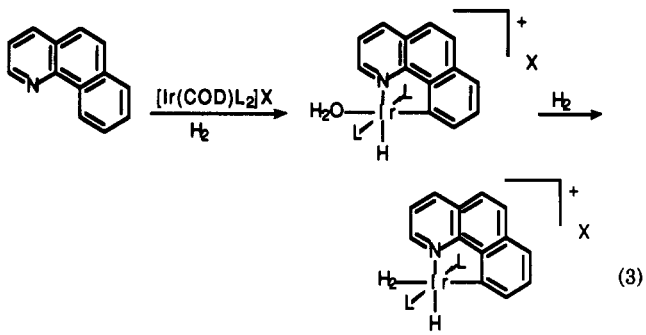

(3)

Results

The 2,6-diarylpyridine ligands ($diarpyH_2$) might be expected to doubly orthometalate. However, we find that they cyclometalate only once to form **2** (eq 4), rare exam-

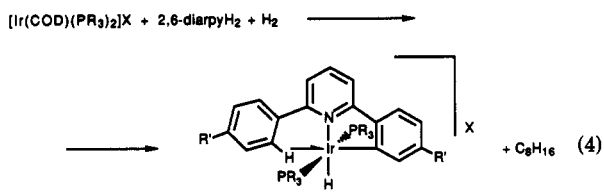

(4)

2

2a: PR_3 = PPh_3; R' = H; X = SbF_6
2b: PR_3 = $P(p\text{-}C_6H_4CH_3)_3$; R' = H; X = SbF_6
2c: PR_3 = $P(4\text{-}C_6H_4F)_3$; R' = H; X = BF_4
2d: PR_3 = PPh_2Me; R' = H; X = SbF_6
2e: PR_3 = P-n-Bu_3; R' = H; X = SbF_6
2f: PR_3 = PPh_3; R' = Me; X = SbF_6

ples of complexes bearing both aryl M–C and agostic C–H···M bonds. They resemble the cyclometalated product of eq 3, but the H_2 ligand is replaced in **2** by an agostic C–H bond. In solution, the agostic and metalated phenyl groups interconvert rapidly at room temperature by what is apparently a facile and reversible oxidative addition/reductive elimination of the M···H–C(aryl) and M–C(aryl) units. By cooling the sample, we were able to freeze this dynamic process and observe decoalescence in the ^1H

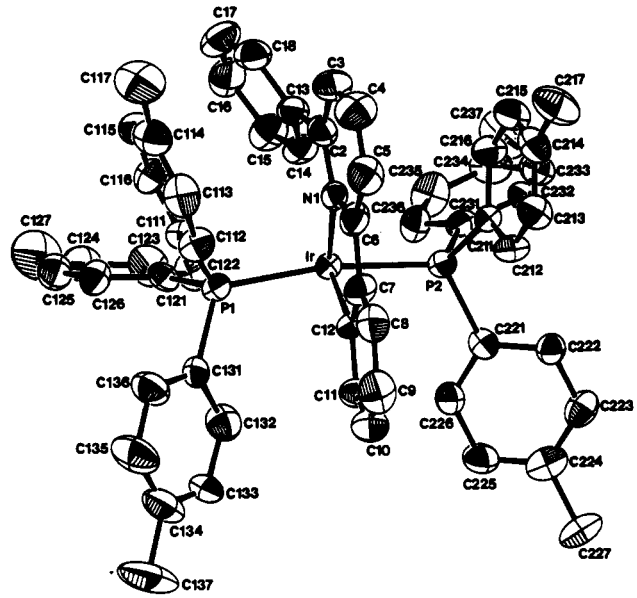

Figure 1. Diagram of the crystal structure of $[Ir(diphpyH)H\{P(p\text{-}C_6H_4CH_3)_3\}_2]SbF_6$ (**2b**) as determined by single-crystal X-ray diffractometry.

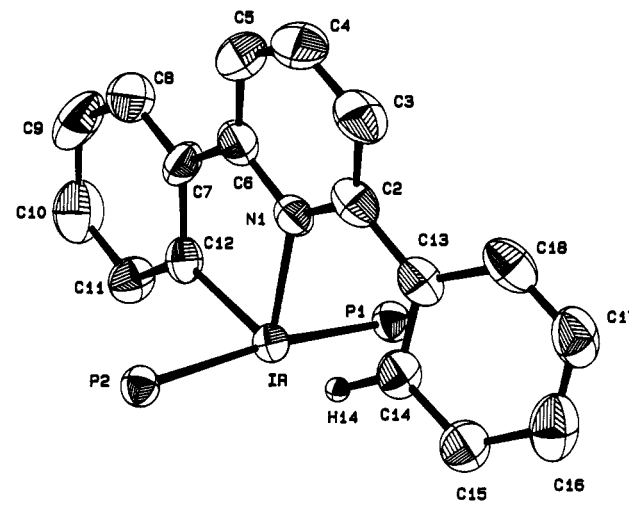

Figure 2. Simplified diagram of **2b**, showing the arrangement of the diphpyH ligand.

NMR spectra, as described below.

$[(COD)Ir(PR_3)_2]X$ (**1**), reacts with 2,6-diphenylpyridine ($diphpyH_2$) or 2,6-di-*p*-tolylpyridine ($ditolpyH_2$) under H_2 at 0 °C to give cyclooctane and complexes **2a–f** as air-stable yellow solids (eq 4). When dissolved, the complexes are only stable in chlorinated solvents (CH_2Cl_2, $CHCl_3$). They decompose in coordinating solvents such as acetone, THF, or alcohols. Even in $CHCl_3$ or CH_2Cl_2, solutions of **2c,e** slowly decomposed in air.

The solid-state structure of one of these compounds, **2b**, was determined by X-ray crystallography. The crystal data, positional parameters, temperature factors, and relevant distances and angles are given in Tables I–III. Figure 1 shows the coordination sphere of the metal in **2b**. The two $P(p\text{-}C_6H_4CH_3)_3$ groups are mutually trans. The diphpyH ligand (Figure 2) is bound through the N atom and an orthometalated phenyl ring (Ir–C = 2.02 Å). The other phenyl ring shows an agostic interaction of one ortho C–H bond with the metal. The key pieces of evidence are the Ir–C14 = 2.69 Å and Ir–H14 = 1.92 Å (estimated using C–H = 1.1 Å) distances, which are much too short for a nonbonded group.[8] The pyridine and the orthometalated ring are almost coplanar (torsion angle 7°), while the

(10) Dolcetti, G.; Hoffman, N. W. *Inorg. Chim. Acta* **1974**, *9*, 269.
(11) Halpern, J. *Inorg. Chim. Acta* **1985**, *100*, 41.
(12) (a) Crabtree, R. H.; Lavin, M.; Bonneviot, L. *J. Am. Chem. Soc.* **1986**, *108*, 4032. (b) Lavin, M.; Holt, E. M.; Crabtree, R. H. *Organometallics* **1989**, *8*, 99.

Table I. Crystal Data for 2b

A. Crystal Data	
empirical formula	$C_{59}H_{54}NIrSbF_6$
fw	1266.99
cryst dimens	0.30 × 0.20 × 0.03 mm
cryst system	triclinic
lattice params	a = 11.072 (2) Å
	b = 14.450 (2) Å
	c = 17.227 (2) Å
	α = 92.76 (1)°
	β = 105.04 (1)°
	γ = 95.00 (1)°
	V = 2644 (1) Å^3
space group	$P\bar{1}$ (No. 2)
Z	2
D_{calc}	1.591 g/cm^3
F_{000}	1254
μ(Mo Kα)	31.36 cm^{-1}
B. Intensity Measurements	
diffractometer	Enraf Nonius CAD4
radiation	Mo Kα (λ = 0.710 69 Å)
temp	room temp
take-off angle	2.8°
$2\theta_{max}$	50.0°
no. of reflcns measd	tot.: 9783
	unique: 9265 (R_{int} = 0.040)
corrs	Lorentz-polarization
	abs[a] (transm factors 0.88–1.17)
C. Structure Solution and Refinement	
struct solution	direct methods
refinement	full-matrix least squares
function minimized	$\sum w(\|F_o\| - \|F_c\|)^2$
least-squares weights	$4F_o^2/\sigma^2(F_o^2)$
p factor	0.03
no. of observns $I \geq 3\sigma$ (I)	5827
no. of var	601
reflcn/param ratio	9.70
residuals	
$R = \sum\|\|F_o\| - \|F_c\|\|/\|F_o\|$	0.052
$R_w = [\sum w(\|F_o\| - \|F_c\|)^2/\sum wF_o^2]^{1/2}$	0.053[b]
goodness of fit indicator	1.50[c]
max shift/error in final cycle	0.23
max peak in final diff map	1.16 e/Å^3
min peak in final diff map	−1.47 e/Å^3

[a] Reference 23. [b] Reference 24. [c] Reference 25.

agostic ring is tilted (torsion angle 24°). The geometry of the ligands and the stoichiometry of the complex suggest the presence of a hydride trans to the N atom of diphpyH; nonetheless, this hydride could not be detected in the diffraction experiment. The IR spectra of **2** confirm the presence of an Ir–H group, a ν_{Ir-H} band being seen between 2110 and 2140 cm^{-1}.

2a–e show dynamic behavior in solution in the NMR time scale consistent with the equilibrium represented in eq 5. In all cases the ^{31}P NMR spectra recorded at 298

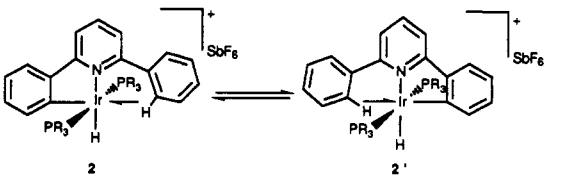

2 2' (5)

K show only one resonance consistent with a trans arrangement of the phosphines, as observed in the solid state. No hydride signals are observed at room temperature by ^{1}H NMR spectroscopy, and several broad resonances appear in the aromatic region. Variable-temperature ^{1}H NMR spectra were recorded for complex **2a**. The spectrum at 223 K, shown in Figure 3, indicates that the Ir–H group is cis to two equivalent phosphines (δ −12.4, t, $^2J_{H-P}$ = 14.5 Hz). As the temperature is raised, this resonance broadens until it becomes indistinguishable from the baseline. The aromatic region simplifies considerably at 298 K. This is more clearly seen by ^{13}C NMR spectroscopy: each member of the pair of diphpyH resonances observed at 218 K coalesce at 298 K. This means that the diphpyH ligand changes from an unsymmetric arrangement to a time-averaged symmetric one as the temperature is raised.

Table II. Important Bond Angles (deg) and Distances (Å) for 2b

Ir–P1	2.335 (3)	C6–C7	1.43 (1)
Ir–P2	2.342 (3)	C7–C8	1.37 (1)
Ir–N1	2.094 (8)	C7–C12	1.45 (1)
Ir–C12	2.01 (1)	C8–C9	1.39 (2)
Ir–C14	2.69 (1)	C9–C10	1.36 (2)
Ir–H14	1.920	C10–C11	1.38 (2)
P1–C111	1.81 (1)	C11–C12	1.37 (1)
P1–C121	1.82 (1)	C13–C14	1.40 (1)
P1–C131	1.83 (1)	C12–C18	1.41 (1)
P2–C211	1.80 (1)	C14–C15	1.38 (2)
P2–C221	1.83 (1)	C15–C16	1.39 (2)
P2–C231	1.83 (1)	C16–C17	1.38 (2)
N1–C2	1.35 (1)	C17–C18	1.38 (2)
N1–C6	1.37 (1)	Sb–F1	1.87 (2)
C2–C3	1.40 (2)	Sb–F5	1.77 (1)
C2–C13	1.48 (2)	Sb–F4	1.80 (2)
C3–C4	1.39 (2)	Sb–F6	1.70 (2)
C4–C5	1.34 (2)	Sb–F2	1.89 (2)
C5–C6	1.40 (2)	Sb–F3	1.85 (2)
P1–Ir–P2	169.1 (1)	N1–C6–C7	114 (1)
P1–Ir–N1	95.4 (2)	C5–C6–C7	126 (1)
P1–Ir–C12	91.3 (3)	C6–C7–C8	123 (1)
P2–Ir–N1	95.0 (2)	C6–C7–C12	117.3 (9)
P2–Ir–C12	87.2 (3)	C8–C7–C12	120 (1)
N1–Ir–C12	80.8 (4)	C7–C8–C9	121 (1)
H14–Ir–C14	15.67	C8–C9–C10	119 (1)
Ir–P1–C111	110.4 (3)	C9–C10–C11	121 (1)
Ir–P1–C121	116.6 (3)	C10–C11–C12	122 (1)
Ir–P1–C131	115.1 (3)	Ir–C12–C7	112.7 (7)
Ir–P2–C211	111.9 (3)	Ir–C12–C11	130.0 (8)
Ir–P2–C221	116.7 (3)	C7–C12–C11	117.3 (9)
Ir–P2–C231	113.6 (3)	C2–C13–C14	122 (1)
Ir–N1–C2	125.2 (7)	C2–C13–C18	121 (1)
Ir–N1–C6	114.9 (7)	C14–C13–C18	117 (1)
C2–N1–C6	119.8 (9)	C13–C14–C15	121 (1)
N1–C2–C3	122 (1)	Ir–C14–H14	31.74
N1–C2–C13	116 (1)	C14–C15–C16	121 (1)
C3–C2–C13	122 (1)	C15–C16–C17	119 (1)
C2–C3–C4	117 (1)	C16–C17–C18	121 (1)
C3–C4–C5	122 (1)	C13–C18–C17	121 (1)
C4–C5–C6	120 (1)	C14–H14–Ir	132.59
N1–C6–C5	120 (1)		

The low-temperature spectra reflect a solution structure similar to that found in the solid state, but at high temperature the fluxional process of eq 5 accounts for the equivalence of the two diphpyH phenyl rings and the disappearance of the hydride signal. No other species were detected. The possibility that a protic impurity might play a role was tested by adding D_2O to a $CHCl_3$ solution of **2**, but no deuterium incorporation was seen by ^{2}H NMR spectroscopy.

The equilibration rates for **2a–f** depend mainly on the basicity of the coordinated phosphine. The process is equally fast for **2a–c** and **2f**, which contain aromatic phosphines and either diphpyH or ditolpyH, and hydride coalescence takes place at 263 K. For **2d**, with contains the more basic PPh_2Me, decoalescence occurs at 223 K, and **2e**, with P-*n*-Bu_3, was the most fluxional, no hydride coalescence being seen down to 183 K.

The exchange process was studied in detail for **2f** by looking at the coalescence of the two Ar*Me* groups in the pyridine ligand. This gave an activation energy of 12.3 kcal

Table III. Positional Parameters and Temperature Factors (Å²) for 2b

atom	x	y	z	B(eq)
Ir	0.027021 (43)	0.217507 (32)	0.271614 (27)	2.38 (2)
P1	−0.10695 (26)	0.22877 (20)	0.14384 (16)	2.7 (1)
P2	0.17647 (26)	0.23503 (19)	0.39697 (16)	2.7 (1)
N1	−0.00174 (77)	0.07213 (55)	0.26915 (47)	2.8 (3)
C2	−0.0948 (11)	0.02372 (79)	0.29241 (62)	3.6 (5)
C3	−0.1015 (12)	−0.07345 (86)	0.29505 (76)	4.8 (6)
C4	−0.0075 (13)	−0.11813 (84)	0.27306 (82)	5.0 (6)
C5	0.0821 (12)	−0.07118 (88)	0.24718 (75)	4.7 (6)
C6	0.0860 (10)	0.02591 (79)	0.24470 (65)	3.5 (5)
C7	0.17305 (95)	0.08489 (79)	0.21546 (65)	3.3 (5)
C8	0.2592 (11)	0.05130 (83)	0.17978 (70)	4.2 (5)
C9	0.3404 (12)	0.1111 (11)	0.15115 (75)	5.1 (6)
C10	0.3356 (12)	0.2049 (10)	0.16031 (74)	4.8 (6)
C11	0.2489 (10)	0.24109 (77)	0.19492 (64)	3.4 (5)
C12	0.16620 (91)	0.18465 (74)	0.22354 (61)	2.9 (4)
C13	−0.1943 (10)	0.07818 (79)	0.30836 (60)	3.4 (5)
C14	−0.1724 (10)	0.17434 (85)	0.32944 (64)	3.5 (5)
C15	−0.2686 (12)	0.22568 (89)	0.33805 (70)	4.5 (6)
C16	−0.3906 (12)	0.1830 (12)	0.32531 (74)	5.5 (7)
C17	−0.4127 (12)	0.0883 (11)	0.30637 (78)	5.2 (6)
C18	−0.3174 (12)	0.03657 (86)	0.29837 (67)	4.4 (5)
C111	−0.18121 (97)	0.11470 (69)	0.10024 (59)	2.8 (4)
C112	−0.1138 (10)	0.05102 (78)	0.07376 (65)	3.6 (5)
C113	−0.1638 (13)	−0.04221 (87)	0.05690 (68)	4.5 (6)
C114	−0.2799 (13)	−0.07308 (88)	0.06644 (68)	4.5 (6)
C115	−0.3484 (11)	−0.00851 (92)	0.09077 (69)	4.3 (5)
C116	−0.3016 (10)	0.08554 (78)	0.10825 (64)	3.6 (5)
C117	−0.3323 (15)	−0.17544 (88)	0.05272 (85)	6.8 (7)
C121	−0.23359 (97)	0.30295 (71)	0.13808 (59)	2.8 (4)
C122	−0.2323 (11)	0.36516 (85)	0.20164 (68)	4.1 (5)
C123	−0.3299 (13)	0.42261 (89)	0.19385 (77)	5.0 (6)
C124	−0.4269 (12)	0.41970 (90)	0.12717 (88)	4.7 (6)
C125	−0.4237 (12)	0.35992 (85)	0.06207 (77)	4.5 (5)
C126	−0.3293 (10)	0.30121 (75)	0.06783 (68)	3.6 (5)
C127	−0.5334 (15)	0.4798 (11)	0.1202 (10)	7.8 (8)
C131	−0.03114 (93)	0.27939 (78)	0.07063 (63)	3.2 (5)
C132	0.0421 (12)	0.36537 (81)	0.09547 (70)	4.3 (5)
C133	0.0971 (11)	0.40873 (89)	0.03947 (78)	4.6 (6)
C134	0.0793 (13)	0.3738 (11)	−0.03645 (86)	5.4 (7)
C135	0.0028 (15)	0.2903 (11)	−0.06030 (77)	6.2 (7)
C136	−0.0536 (12)	0.24494 (87)	−0.00744 (72)	4.6 (6)
C137	0.1428 (17)	0.4217 (12)	−0.0937 (10)	9 (1)
C211	0.22745 (90)	0.12534 (68)	0.42973 (57)	2.6 (4)
C212	0.3245 (10)	0.08837 (75)	0.40696 (66)	3.4 (5)
C213	0.3469 (11)	−0.00318 (84)	0.41854 (68)	4.0 (5)
C214	0.2722 (12)	−0.06197 (82)	0.45081 (67)	4.2 (5)
C215	0.1756 (12)	−0.02556 (87)	0.47462 (70)	4.4 (6)
C216	0.1526 (10)	0.06604 (78)	0.46444 (67)	3.6 (5)
C217	0.2934 (14)	−0.16290 (91)	0.45861 (83)	6.0 (7)
C221	0.31960 (98)	0.31284 (68)	0.40450 (59)	2.7 (4)
C222	0.42953 (98)	0.30337 (74)	0.46377 (63)	3.2 (4)
C223	0.5350 (11)	0.36395 (80)	0.47011 (71)	3.9 (5)
C224	0.5334 (11)	0.43527 (83)	0.42073 (79)	4.2 (5)
C225	0.4245 (12)	0.44715 (79)	0.36413 (72)	4.2 (5)
C226	0.3186 (10)	0.38679 (82)	0.35706 (62)	3.8 (5)
C227	0.6523 (11)	0.50052 (84)	0.42673 (79)	4.9 (6)
C231	0.11773 (93)	0.28443 (71)	0.47848 (63)	3.0 (4)
C232	0.1724 (10)	0.27083 (76)	0.55959 (63)	3.3 (5)
C233	0.1301 (12)	0.31244 (87)	0.62052 (70)	4.4 (5)
C234	0.0316 (13)	0.36791 (88)	0.60410 (77)	4.7 (6)
C235	−0.0182 (12)	0.38331 (87)	0.52369 (81)	4.9 (6)
C236	0.0249 (10)	0.34339 (81)	0.46148 (65)	3.7 (5)
C237	−0.0177 (15)	0.4092 (10)	0.66846 (83)	6.8 (8)
Sb	0.55498 (11)	0.243715 (74)	0.758563 (64)	6.63 (6)
F1	0.3883 (16)	0.2356 (11)	0.76444 (95)	18.0 (5)
F5	0.6046 (13)	0.2946 (10)	0.85860 (85)	15.6 (4)
F4	0.7133 (15)	0.2325 (11)	0.75328 (92)	17.4 (5)
F6	0.5494 (17)	0.3449 (13)	0.7121 (11)	21.0 (6)
F2	0.4933 (15)	0.1774 (11)	0.65658 (93)	17.5 (5)
F3	0.5637 (17)	0.1314 (13)	0.8055 (11)	21.0 (6)

mol^{-1} (257 K) for the equilibrium shown in eq 5.[13]

Reactions of **2a** with donor ligands like CO or CH_3CN lead to displacement of the agostic C–H group to give orthometalated hydrides **3** and **4** (eq 6). The presence of

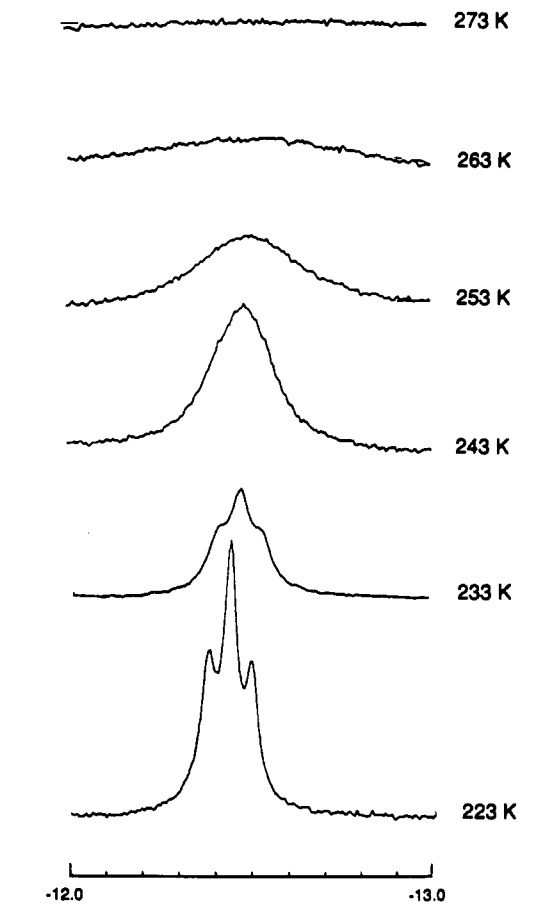

Figure 3. Hydride region of the variable-temperature ^1H NMR spectra (250 MHz, $CDCl_3$) of $[Ir(diphpyH)H(PPh_3)_2]SbF_6$ (**2a**).

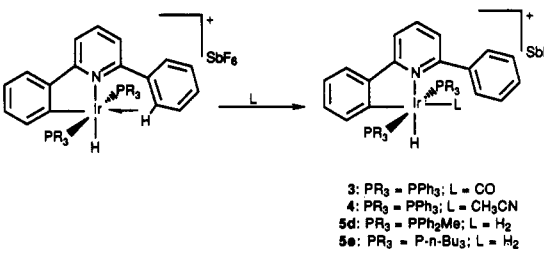

the added ligand is established by IR spectroscopy (**3**, ν_{CO} = 2050 cm^{-1}) or ^1H NMR spectroscopy (**4**, δ 1.29, coordinated CH_3CN). The ^1H NMR spectra in the hydride region show resonances at δ −16.4 (t, $^2J_{H-P}$ = 13 Hz, **3**) and δ −19.2 (t, $^2J_{H-P}$ = 15.5 Hz, **4**), chemical shifts that correspond to Ir–H trans to N and $^2J_{H-P}$ values consistent with Ir–H cis to the two equivalent PPh_3 groups. The proposed stereochemistry is also consistent with that found crystallographically for the benzoquinoline analogue.[8] Complex **2a** does not react with N_2.

2d,e react with H_2 in a similar fashion, the H_2 acting as a ligand to displace the agostic aryl C–H, and form the dihydrogen derivatives $[Ir(diphpyH)H(\eta^2\text{-}H_2)(PR_3)_2]$ (**5d**, PR_3 = PPh_2Me; **5e**, PR_3 = P-*n*-Bu_3). Systems in which both an H_2 and C–H bond have both been shown to bind at the same site are still rather rare.[3,4a,b] At 233 K the H_2 resonance appears as a broad signal at δ −3.86 (**5d**) and −5.12 (**5e**); the terminal hydride resonance is a triplet at δ −17.61 ($^2J_{H-P}$ = 15.3 Hz) for **5d** or δ −18.50 ($^2J_{H-P}$ = 15 Hz) for **5e**. When D_2 is bubbled through a $CDCl_3$ solution of **5**, exchange between the D_2 and the *cis*-H–Ir–(η^2-H_2) occurs; $^1J_{H-D}$ values of 33.5 Hz (**5d**) and 32 Hz (**5e**) were

(13) Günter, H. *NMR Spectroscopy*; J. Wiley & Sons: New York, 1980; p 241.

Scheme I

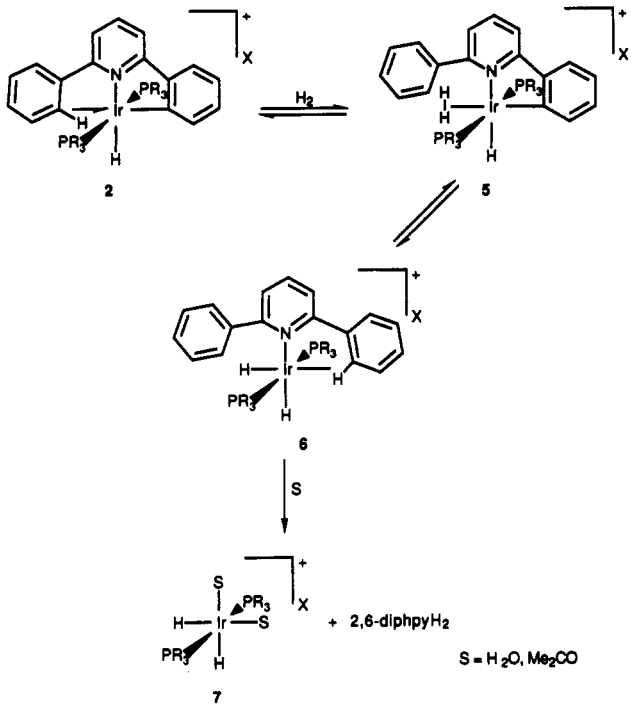

found for Ir–(η^2-HD), confirming the nonclassical formulation.

On longer reaction with H_2, complexes **2a–c** and **2f** not only give η^2-H_2 complexes but can also undergo hydrogenolysis of the Ir–Ar bond (see Scheme I). For example, reaction of **2a** with H_2 at 0 °C for 5 min in CD_2Cl_2 or $CDCl_3$ gives a mixture of the dihydrogen complex **5a** and the hydrogenolysis product **6a**. At 233 K, resonances appear in the hydride region at δ −3.4 (b) and −16.24 (t, $^2J_{H-P}$ = 13.7 Hz), which are assigned to the dihydrogen complex **5a**, and at δ −24.1 (b), corresponding to **6a**. The formulation of **6a** as a dihydride is supported by the variable-temperature behavior of the δ −24.1 resonance: at 298 K it appears as a triplet at δ −24.7 ($^2J_{H-P}$ = 17.6 Hz); at 173 K it has decoalesced into two broad signals of equal intensity at δ −19.8 and −27.0. The facile interconversion between the two hydrides (ΔG^* = 8 kcal mol^{-1}, 193 K) is unusual in an octahedral complex and is most probably due to the presence of a labile agostic bond. Loss of this ligand, together with formation of an H_2 complex, would lead to a 4-coordinate Ir(I) species; reversal of these steps would lead to the observed fluxionality.

The intensity ratio of the resonances of the dihydrogen complex and the dihydride is temperature dependent, and this equilibrium was studied in detail for **5b** = **6b** (see below). The hydrogenolysis is reversible because **2a** is recovered by bubbling Ar through the solution. If H_2 reacts with **2a** for as long as 15 min, the diphpyH_2 is entirely displaced from the metal. The reaction is now irreversible, probably because the new Ir species precipitates as a white solid. This was identified as the known[14,15] $[Ir(H)_2(PPh_3)_2(H_2O)_2]SbF_6$ (**7**). In a reaction similar to ones we have seen before,[8] residual H_2O present in the deuterated solvent presumably coordinates after loss of diphpyH_2 from the metal. The irreversibility of the reaction is probably simply a result of the insolubility of **7**.

The reaction of **2a** with H_2 in the presence of NEt_3 did not lead to the formation of the same hydride species **6a**, so **6a** is not the product of simple deprotonation of the H_2 ligand, which would give $[Ir(diphpyH\text{-}N,C)(H)_2(PPh_3)_2]$. Only reversible hydrogenolysis can explain the spectral data and the reactivity pattern observed, and we propose the pathway shown in Scheme I, in which H_2 causes reversible Ir–Ar bond cleavage.

Table IV shows the equilibrium constants for **5** and **6** at 233 K. They were calculated from the intensities of the hydride signals; a pulse delay of at least five T_1's was used to ensure complete relaxation. The temperature dependence of the equilibrium for **5b** = **6b** was analyzed over a 60 °C temperature range. An Eyring plot gave ΔH = 1.6 ± 0.4 kcal mol^{-1} and ΔS = 8 ± 2 cal mol^{-1} K^{-} The positive entropy is probably a result of the greater freedom of motion of the agostic aryl group in **6b** compared to the Ir–Ar bond of **5b**.

Table IV. Constants for the Equilibrium 5/6 at 233 K

complexes[a]	K_{eq}[b]	complexes[a]	K_{eq}[b]
a (PPh_3, diphpyH)	3.48 ± 0.3	**c** ($P(p\text{-}C_6H_4F)_3$, diphpyH)	2.73 ● 0.2
b ($P(p\text{-}C_6H_4CH_3)_3$, diphpyH)	1.86 ± 0.1	**f** (PPh_3, ditolpyH)	10.25 ± 1

[a] The letters below refer to eq 2. [b] K_{eq} is defined as [6]/[5] and determined by ^{1}H NMR integration of the hydride resonances of **5** and **6**.

Discussion

Double metalation of a ligand to one metal center is relatively uncommon.[16] 2,6-Dialkylpyridines (dialkpyH_2) can metalate twice to form *trans*-[M(dialkpy-*N,C,C'*)L] (M = Pt, Pd),[16a,b] but 2,6-diarylpyridines have failed to do so either with these metals or with Rh and Ir.[17] Two reasons have been advanced: steric inhibition of the approach of the second phenyl ring to the metal center after the first metalation and strain in the polycyclic ring system of the dimetalation product. These arguments are difficult to reconcile with the presence of similar ring systems in other stable compounds. For example, [M(diphpy-*N,C,C'*)L] (M = Pd, Pt; L = Py, SEt_2) has been synthesized from $[MCl_2(SEt_2)_2]$ and Li_2diphpy.[16c] It is almost certainly dimetalated, although structural characterization was not reported. The crystal structure of [Pd(terpy)Cl]Cl[18] shows coordination of the three nitrogens, in an arrangement analogous to the one expected for diphpy-*N,C,C'* without any unusual bond angles or distances that would indicate strain.

It is now clear that the electronic characteristics of the metal center play the most important role in allowing the second metalation. In our system the second phenyl ring is close enough to the metal center to be able to interact with it in an agostic fashion, yet the metal center does not

(14) ^{1}H NMR ($(CD_3)_2CO$): δ −27.9t (J_{P-H} = 15.2). In acetone-d_6, the complex $[Ir(H)_2(PPh)_3\{(CD_3)_2CO\}_2]SbF_6$ is most probably formed; the identity of **7** was confirmed by independent synthesis.[15]

(15) Crabtree, R. H.; Demou, P. C.; Eden, D.; Mihelcic, J. M.; Parnell, C. A.; Quirk, J. M.; Morris, G. M. *J. Am. Chem. Soc.* **1982**, *104*, 6994.

(16) (a) Newkome, G. R.; Kawato, T.; Kohli, D. K.; Puckett, W. E.; Olivier, B. D.; Chiari, G.; Fronczek, F. R.; Deutsch, W. A. *J. Am. Chem. Soc.* **1981**, *103*, 3423. (b) Newkome, G. R.; Kohli, D. K.; Fronczek, F. R. *J. Am. Chem. Soc.* **1982**, *104*, 994. (c) Cornioley-Deuschel, C.; Ward, T.: Von Zelewsky, A. *Helv. Chim. Acta* **1988**, *71*, 130. (d) Carter, S. T.; Clegg, W.; Gibson, V. C.; Kee, T. P.; Sanner, R. D. *Organometallics* **1989**, *8*, 253. (e) Cloke, F. G. N.; Green, J. C.; Green, M. L. H.; Morley, C. P. *J. Chem. Soc., Chem. Commun.* **1985**, 945. (f) Baltensperger, U.; Günter, J. R.; Kägi, S.; Kahr, G.; Marty, W. *Organometallics* **1983**, *5*, 571.

(17) (a) Selbin, J.; Abboud, K.; Watkins, S. F.; Gutierrez, M. A.; Fronczek, F. R. *J. Organomet. Chem.* **1983**, *241*, 259. (b) Selbin, J.; Gutierrez, M. A. *J. Organomet. Chem.* **1983**, *246*, 95.

(18) Intille, G. M.; Pfluger, C. E.; Baker, W. A., Jr. *J. Cryst. Mol. Struct.* **1973**, *3*, 47.

Scheme II

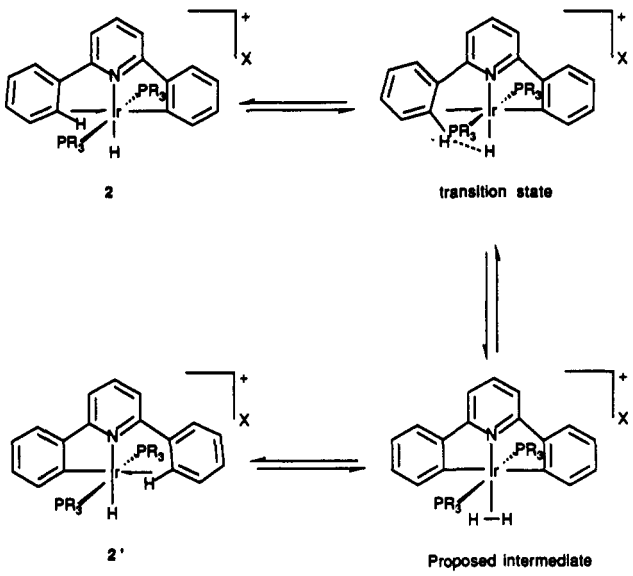

oxidatively add this second C–H bond. The existence of the dihydrogen derivatives $[Ir(diphpyH)H(\eta^2\text{-}H_2)(PR_3)_2]$ (**5**) and other η^2-H_2 complexes in similar systems[12a] indicates that the Ir(III) center is not basic enough to break the H–H bond to give a thermodymamically stable dihydride, and for the same reason it is not expected to break the *o*-C–H bond of the second phenyl ring.

The rate of the equilibrium of eq 5 depends on the basicity of the phosphine coordinated to the metal center: P-*n*-Bu_3 > PPh_2Me > PAr_3. Assuming steric effects are unimportant, the higher σ-donor (or reduced π-acceptor) ability of the alkylphosphines make the Ir more basic and leads to more rapid cleavage of the agostic C–H bond. This suggests that the exchange is associative and goes via the dimetalated species rather than dissociative via the bis agostic system because a more basic metal is expected to give faster oxidative addition but slower reductive elimination. This in turn means that the $\Delta G^{\ddagger}$ of 12.3 kcal/mol measured for eq 5 represents the activation energy for the oxidative addition. The associative process could go in one of two ways, either by full oxidative addition to give the iridium(V) dihydride or it could avoid oxidative addition if it went via an iridium(III) dihydrogen complex (Scheme II). The latter is a strong possibility by analogy with the work of Luo et al.,[4c] who have shown that a rhenium dihydrogen hydride exchanges via an (H_3) intermediate or transition state, thus avoiding oxidative addition. A reviewer has suggested a concerted process in which the terminal hydride inserts into the C–M bond as the agostic C–H undergoes oxidative addition.

Hydrogenolysis is observed when complexes **2a–c** and **2f** (PR_3, R = aryl) react with H_2, while only the η^2-H_2 derivatives $[Ir(diphpyH)H(\eta^2\text{-}H_2)(PR_3)_2]$ (**5d,e**) are formed from **2d** (PR_3 = PPh_2Me) or **2e** (PR_3 = P-*n*-Bu_3) and H_2. This observation means that species **5** are favored for P-*n*-Bu_3 and PPh_2Me and the hydrogenolysis product **6** is favored for PAr_3 (see Scheme I). Nevertheless the dihydrogen complexes **5** are only slightly more stable than the dihydrides **6**, as shown by the small value found for ΔH in the equilibrium **5** = **6**. The more basic the phosphine, the more the equilibrium disfavors the hydrogenolysis product, no doubt because oxidative addition of the strongly electronegative aryl group is preferred for a more basic metal. As can be seen in Table IV the hydrogenolysis product **6** is favored for the less electronegative ditolpyH (**5f** = **6f**, K_{eq} = 10.25 ± 1) over the parent diphpyH (**5a** = **6a**, K_{eq} = 3.48 ± 0.3) system, consistent with the arguments above.

The hydrogenolysis product is probably formed by heterolytic activation of the H_2 complex (eq 2a), but a reductive elimination route via a terminal hydride (eq 2b) cannot be excluded. Although the H_2 ligand in **5** is trans to the Ir–Ar bond to be cleaved, there is rapid exchange between this H and the cis H_2, so the H_2 ligand is probably cis to the Ir–Ar bond for a significant fraction of the time.

The strength of an agostic interaction in comparison with other systems can be estimated using the r_{bp} parameter defined by Crabtree et al.[8] From the structural parameters found for **2b**, we can assign an r_{bp} value of 0.83 for our system, which corresponds to a relatively strong interaction. A plot of r_{bp} versus the M–H–C angle gives a curve which defines the trajectory for the oxidative addition of C–H to the metal.[8] The values for our complex fall close to this curve. The phenyl group bearing the agostic C–H bond is tilted 24° with respect to the pyridine ring, while the other phenyl ring is almost in the same plane (torsion angle 7°). The torsion of the agostic ring changes the orientation of the *o*-C–H bond so it forms an Ir–H–C angle of 132.6°. If the three rings had been coplanar the M–H–C angle would have been approximately 160°; rotation of the ring is favorable because it leads to a decrease in the angle, making it closer to the preferred angle of 120° given by the trajectory study.

Conclusions

The 2,6-diarpyH_2 complexes **2a–f** contain an agostic C–H bond trans to an M–C group. Electronic rather than steric effects seem to prevent the formation of a doubly metalated diarpy ligand. Rapid interconversion between C–M···H–C and C–H···M–C is observed at room temperature, a reaction which involves oxidative addition of the agostic C–H bond and reductive elimination of the aryl hydride. This is an unusual example of reversible metalation of an agostic group under mild conditions. The exchange reaction seems to go via the doubly metalated species, oxidative addition of the agostic C–H bond being the first step, as shown by the lowering of $\Delta G^{\ddagger}$ observed as the electron density on the metal rises. Iridium(V) and iridium(III) dihydrogen complexes are plausible intermediates.

The importance of the electron density on the metal is shown in the reactions of complexes **2** with H_2: only the dihydrogen derivatives **5** are formed for the complexes with the more electron-rich centers (**2d–e**), while hydrogenolysis to give the dihydrides **6** is also observed for **2a–c** and **2f**. Heterolytic cleavage of the Ir–C bond is favored by the presence of less basic phosphines.

The hydrogen complex **5** appears to be the key intermediate in the hydrogenolysis of the Ir–Ar bond by H_2.

Experimental Section

^1H, ^{13}C, ^{31}P, and ^2D NMR spectra were recorded on a Bruker WM 250 or Bruker WM 500 instrument. ^1H and ^{13}C chemical shifts were measured with reference to the residual solvent resonances; ^{31}P chemical shifts were measured with external 85% H_3PO_4 as reference; ^2D chemical shifts were measured using C_6D_6 as a reference. IR spectra were recorded on a Nicolet 5-SX FT-IR spectrometer. Microanalyses were carried out by Galbraith Laboratories, Inc.

Reagents were purchased from Aldrich Chemical Co. $[Ir(COD)(PR_3)_2]X$[19] was prepared by published procedures.

(19) (a) Haines, L. M.; Singleton, E. *J. Chem. Soc., Dalton Trans.* **1972**, 1891. (b) Crabtree, R. H.; Morris, G. E. *J. Organomet. Chem.* **1977**, *135*, 395.

Hydro[2-(6-phenyl-2-pyridinyl)phenyl-*C*,*N*]bis(triphenylphosphine)iridium(III) Hexafluoroantimonate (2a). $[Ir(COD)(PPh_3)_2]SbF_6$ (0.445 g, 0.42 mmol) was dissolved in CH_2Cl_2 (20 mL), and 2,6-diphpy (0.097 g, 0.42 mmol) was added to the red solution. The mixture was cooled to 0 °C, and H_2 was bubbled through it for 5 min. During this time the solution turned from red to yellow. The solvent was evaporated to ca. 2 mL, and diethyl ether (10 mL) was added. A yellow product precipitated, which was filtered out, washed with Et_2O, and dried in vacuo (0.424 g, 85%). Recrystallization from CH_2Cl_2/Et_2O afforded analytically pure material. Anal. Calcd for $C_{53}H_{43}F_6IrNP_2Sb$: C, 53.77; H, 3.66; N, 1.18. Found: C, 53.88; H, 3.67; N, 1.18. IR (KBr pellet): ν_{Ir-H} 2141 cm^{-1}. $^{31}P\{^1H\}$ NMR (500 MHz, $CDCl_3$, 298 K): δ 21.6. ^1H NMR (500 MHz, CD_2Cl_2, 218 K): δ 7.53 (t, $^3J_{H-H}$ = 7.8 Hz, 1 H, H4), 7.35–7.23 (m, 33 H), 7.15 (t, $^3J_{H-H}$ = 7.2 Hz, 1 H), 7.10 (d, $^3J_{H-H}$ = 8 Hz, 1 H), 6.97 (d, $^3J_{H-H}$ = 7.6 Hz, 1 H), 6.74 (t, $^3J_{H-H}$ = 6 Hz, 1 H), 6.61 (d, $^3J_{H-H}$ = 8 Hz, 1 H), 6.27 (t, $^3J_{H-H}$ = 6 Hz, 1 H, H3″), 5.84 (d, $^3J_{H-H}$ = 6.4 Hz, 2 H, H3′ + H2″-agostic), −12.4 (t, $^2J_{H-P}$ = 14.5 Hz, 1 H, Ir–H). ^1H NMR (250 MHz, $CDCl_3$, 298 K): δ 7.70 (t, $^3J_{H-H}$ = 7.5 Hz), 7.50–7.00 (m), 6.90–6.70 (b). ^{13}C NMR (500 MHz, CD_2Cl_2, 218 K): δ 159.98, 156.29, 141.72, 140.70, 138.44 (d, $^1J_{C-H}$ = 161 Hz), 137.47 (d, $^1J_{C-H}$ = 166 Hz), 133.82 (d, $^1J_{C-H}$ = 187 Hz), 132.67 (m, J_{P-C} = 11.3, $^1J_{C-H}$ = 162 Hz, PPh_3 C-ortho), 130.86 (d, $^1J_{C-H}$ = 161 Hz), 130.57 (d, $^1J_{C-H}$ = 162 Hz, PPh_3 C-para), 128.54 (d, $^1J_{C-H}$ = 151 Hz), 128.31 (m, J_{P-C} = 5 Hz, $^1J_{C-H}$ = 163 Hz, PPh_3 C-meta), 128.04 (d, $^1J_{C-H}$ = 50.3 Hz, C-agostic), 127.81 (PPh_3, C-ipso), 123.96 (d, $^1J_{C-H}$ = 166 Hz), 122.65 (d, $^1J_{C-H}$ = 166 Hz), 121.04 (b, Ir–C), 120.56 (d, $^1J_{C-H}$ = 163 Hz), 118.01 (d, $^1J_{C-H}$ = 156 Hz), 117.90 (d, $^1J_{C-H}$ = 156 Hz). $^{13}C\{^1H\}$ NMR (500 MHz, $CDCl_3$, 323 K): δ 159.38 (b), 140.01, 138.19 (b), 133.05 (PPh_3), 130.93 (PPh_3), 130.21 (b), 129.09, 128.86, 128.57 (PPh_3), 121.18 (b), 120.36 (b).

Complexes **2b–f** were prepared by a similar method and in similar yields.

2b. Anal. Calcd for $C_{59}H_{55}F_6IrNP_2Sb$: C, 55.88; H, 4.37; N, 1.10. Found: C, 55.73; H, 4.45; N, 1.12. IR (KBr pellet): ν_{Ir-H} 2112 cm^{-1}. $^{31}P\{^1H\}$ NMR (500 MHz, $CDCl_3$, 298 K): δ 19.99. ^1H NMR (250 MHz, $CDCl_3$, 298 K): δ 7.70 (t, $^3J_{H-H}$ = 8.5 Hz, 1 H), 7.25–6.9 (m), 6.8–6.6 (b, 6 H), 2.33 (s, 18 H, *p*-CH_3).

2c. Anal. Calcd for $C_{53}H_{37}BF_{10}IrNP_2$: C, 55.70; H, 3.26; N, 1.22. Found: C, 55.72; H, 3.30; N, 1.22. IR (KBr pellet): ν_{Ir-H} 2117 cm^{-1}. $^{31}P\{^1H\}$ NMR (500 MHz, $CDCl_3$, 298 K): δ 18.30. ^1H NMR (250 MHz, $CDCl_3$, 298 K): δ 7.75 (t, $^3J_{H-H}$ = 7.7 Hz, 1 H), 7.4–6.8 (m, aromatic).

2d. Anal. Calcd for $C_{43}H_{39}F_6IrNP_2Sb$: C, 48.74; H, 3.71; N, 1.32. Found: C, 48.56; H, 3.83; N, 1.30. IR (KBr pellet): ν_{Ir-H} 2108 cm^{-1}. $^{31}P\{^1H\}$ NMR (500 MHz, $CDCl_3$, 298 K): δ 0.07. ^1H NMR (250 MHz, CD_2Cl_2, 298 K): δ 7.61 (t, $^3J_{H-H}$ = 8 Hz, 1 H), 7.37–7.05 (m, 32 H), 1.60 (t, J_{H-P} = 4 Hz, 6 H).

2e. Anal. Calcd for $C_{41}H_{67}F_6IrNP_2Sb$: C, 46.28; H, 6.35; N, 1.31. Found: C, 45.95; H, 6.31; N, 1.29. IR (KBr pellet): ν_{Ir-H} 2126 cm^{-1}. $^{31}P\{^1H\}$ NMR (500 MHz, $CDCl_3$, 298 K): δ −11.29. ^1H NMR (250 MHz, $CDCl_3$, 298 K): δ 8.2–7.3 (m, diphpyH), 1.20 (m, P-*n*-Bu_3), 1.13 (t, $^3J_{H-H}$ = 7 Hz, P–CH_2–), 0.99 (m, P-*n*-Bu_3), 0.77 (t, $^3J_{H-H}$ = 7 Hz, –CH_3 of P-*n*-Bu_3).

2f. Anal. Calcd for $C_{55}H_{47}F_6IrNP_2Sb$: C, 54.51; H, 3.91; N, 1.15. Found: C, 54.59; H, 3.97; N, 1.18. IR (KBr pellet): ν_{Ir-H} 2130 cm^{-1}. $^{31}P\{^1H\}$ NMR (500 MHz, $CDCl_3$, 298 K): δ 20.72. ^1H NMR (250 MHz, CD_2Cl_2, 298 K): δ 7.56 (t, $^3J_{H-H}$ = 7.8 Hz, 1 H), 7.4–7.1 (m, 37 H), 6.63 (b, 3 H), 1.94 (s, 6 H, CH_3).

Hydro[2-(6-phenyl-2-pyridinyl)phenyl-*C*,*N*]carbonylbis(triphenylphosphine)iridium(III) Hexafluoroantimonate (3). **2a** (95 mg, 0.08 mmol) was dissolved in CH_2Cl_2 (10 mL). CO was passed through the solution at room temperature. In 1 min the solution changed from yellow to colorless. The solvent was evaporated to ca. 0.5 mL. The additon of cold Et_2O (5 mL) led to the precipitation of a white solid (**3**), which was filtered out, washed with cold Et_2O, and dried in vacuo (77 mg, 80%). The product was spectroscopically and analytically pure without further purification. Anal. Calcd for $C_{54}H_{43}F_6IrNOP_2Sb$: C, 53.52; H, 3.58; N, 1.15. Found: C, 53.33; H, 3.61; N, 1.16. IR (KBr pellet): ν_{Ir-H} 2217 cm^{-1}, ν_{CO} 2050 cm^{-1}. $^{31}P\{^1H\}$ NMR (500 MHz, $CDCl_3$, 298 K): δ 5.74. ^1H NMR (250 MHz, $CDCl_3$, 298 K): δ 7.7–6.5 (m, aromatic), −16.45 (t, $^2J_{H-P}$ = 13 Hz, Ir–H). $^{13}C\{^1H\}$ (500 MHz, $CDCl_3$, 298 K): δ −173.68 (t, $^2J_{C-P}$ = 7.9 Hz, CO), −148.34 (t, $^2J_{C-P}$ = 17 Hz, Ir–C).

Hydro[2-(6-phenyl-2-pyridinyl)phenyl-*C*,*N*](acetonitrile)bis(triphenylphosphine)iridium(III) Hexafluoroantimonate (4). **2a** (60 mg, 0.05 mmol) was dissolved in CH_3CN (5 mL), and the solution was stirred at room temperature for 30 min. During this time the solution turned from yellow to colorless. The solvent was evaporated to ca. 0.5 mL, and Et_2O (5 mL) was added. A white product (**4**) precipitated, and it was filtered out, washed with Et_2O, and air dried (55 mg, 90%). The product was spectroscopically and analytically pure without further purification. Anal. Calcd for $C_{55}H_{46}F_6IrN_2P_2Sb$: C, 53.93; H, 3.78; N, 2.28. Found: C, 53.56; H, 3.81; N, 2.26. IR (KBr pellet): ν_{Ir-H} 2217 cm^{-1}. $^{31}P\{^1H\}$ NMR (500 MHz, $CDCl_3$, 298 K): δ 10.47. ^1H NMR (250 MHz, $CDCl_3$, 298 K): δ 7.5–6.3 (m, aromatic), 1.29 (s, CH_3CN), −19.16 (t, $^2J_{H-P}$ = 15.5 Hz).

Reactions of Complexes 2a–f with H_2. Hydro[2-(6-phenyl-2-pyridinyl)phenyl-*C*,*N*](dihydrogen)bis(tri-*n*-butylphosphine)iridium(III) Hexafluoroantimonate (5e). **2e** (10 mg, 0.009 mmol) was dissolved in $CDCl_3$ (0.5 mL). The solution was cooled to 0 °C, and H_2 was passed through for 5 min. During this time the solution became paler. A ^1H NMR spectrum of the solution (250 MHz, 233 K) showed the presence of **5e**: δ −5.12 (b, 2 H, Ir–η^2-H_2), −18.50 (t, $^2J_{H-P}$ = 15 Hz, Ir–H). When a mixture of H_2 and D_2 was bubbled through the solution, the partially deuterated dihydrogen complex, **5e-*d***, was obtained. ^1H NMR (250 MHz, 233 K): δ −5.15 (t, $^1J_{H-D}$ = 32 Hz, Ir–HD).

The reactions of **2a–d** and **2f** with H_2 were carried out in the same way.

5a. ^1H NMR (250 MHz, $CDCl_3$, 233 K): δ −3.4 (b, 2 H, Ir–η^2-H_2), −16.24 (t, 1 H, $^2J_{H-P}$ = 13.7 Hz).

5b. ^1H NMR (250 MHz, CD_2Cl_2, 233 K): δ −3.39 (b, 2 H, Ir–η^2-H_2), −16.44 (t, 1 H, $^2J_{H-P}$ = 13.5), $^1J_{H-D}$ = 29 Hz.

5c. ^1H NMR (250 MHz, $CDCl_3$, 233 K): δ −3.3 (b, 2 H, Ir–η^2-H_2), −16.35 (t, 1 H, $^2J_{H-P}$ = 13 Hz).

5d. ^1H NMR (250 MHz, CD_2Cl_2, 233 K): δ −3.86 (b, 2 H, Ir–η^2-H_2), −17.60 (t, $^2J_{H-P}$ = 15.7), $^1J_{H-D}$ = 33.5 Hz.

5f. ^1H NMR (250 MHz, $CDCl_3$, 233 K): δ −3.4 (b), −16.51 (t).

6a. ^1H NMR (250 MHz, $CDCl_3$, 298 K): δ 8.13–6.37 (b, aromatic), −24.70 (t, $^2J_{H-P}$ = 16.8 Hz, Ir–$(H)_2$).

6b. ^1H NMR (CD_2Cl_2, 250 MHz, 298 K): δ 8.1–6.2 (b, 37 H, aromatic), 2.36 (s, 18 H, *p*-Me), −24.75 (b, 22 H, Ir–$(H)_2$).

6c. ^1H NMR ($CDCl_3$, 250 MHz, 298 K): δ 8.0–6.5 (m, aromatic), −29.45 (t, $^2J_{H-P}$ = 16.8 Hz, Ir–$(H)_2$).

6f. ^1H NMR ($CDCl_3$, 250 MHz, 298 K): δ 7.8–6.2 (m, aromatic), −24.69 (t, $^2J_{H-P}$ = 16.8 Hz, Ir–$(H)_2$).

Study of Equilibrium 5 = 6. Equilibrium constants were determined using the mean of the integration ratios of the hydride signals for **5** and **6** ($(6\{(M-H)_2\}/5(M-H_2)$ and $6\{(M-H)_2\}/5(M-H)$) after complete relaxation (a delay of at least five T_1's was used between pulses). Errors in K_{eq} were estimated as ±10%. The ln K_{eq} vs $1/T$ plot is linear and gave the values for ΔH and ΔS. Uncertainties in the thermodynamic parameters were evaluated by using the method of Markgraf and co-workers.[20]

X-ray Analysis. **2b** was crystallized by slow diffusion of benzene into a CH_2Cl_2 solution of the complex. The compound grew as yellow needles. A suitable crystal of dimensions 0.30 × 0.20 × 0.03 mm was mounted in a random orientation on a glass fiber. Crystal data and details for intensity measurements and structure solution and refinement are given in Table I. The structure was solved using SHELXS86,[21] where the entire non-hydrogen structure was visible in the initial electron density map. All the hydrogen positions were calculated, and for the H atoms temperature factors were assigned which were 20% greater than the value for the attached heavy atom. They were included in the refinement with their structure factor contributions but otherwise not refined. The maximum and minimum peaks on the final difference Fourier map corresponded to 1.16 and −1.47 e/Å^3. There is disorder around the SbF_6. The fluorines were refined isotropically and show residual electron density around F3, F5, and F6, which accounts for the four most intense peaks in the difference Fourier map. All calculations were performed

(20) Petersen R. C.; Markgraf, J. H.; Ross, S. D. *J. Am. Chem. Soc.* **1961**, *83*, 3819.

(21) Sheldrick, G. M. *SHELXS86, Program for Crystal Structure Determination*; University of Cambridge: Cambridge, U.K., 1986.

using the TEXSAN[22] crystallographic software package developed by Molecular Structure Corp.

Acknowledgment. We thank the Spanish Ministry of Education and Science and the Fulbright Comission for a postdoctoral fellowship (A.C.A.) and the NSF for funding.

(22) *TEXSAN: Single Crystal Structure Analysis Software, Version 5.0*; Molecular Structure Corp.: The Woodlands, TX 77381, 1989.
(23) DIFABS: Walker, N.; Stuart, D. *Acta Crystallogr.* **1983**, *A39*, 158. DIFABS defines the average transmission factor to be near unity; therefore, the minimum and maximum transmission factors will be less than and greater than unity, respectively.
(24) Least-squares function minimized: $\sum w(|F_o| - |F_c|)^2$, where $w = 4F_o^2/\sigma^2(F_o)^2$, $\sigma^2(F_o^2) = [S^2(C + R^2B) + (pF_o^2)^2]/(Lp)^2$, S = scan rate, C = total integrated peak count, R = ratio of scan time to background counting time, B = total background count, Lp = Lorentz–polarization factor, and $p = p$ factor.
(25) Standard deviation of an observation of unit weight: $[\sum w(|F_o| - |F_c|)^2/(N_o - N_v)]^{1/2}$, where N_o = number of observations and N_v = number of variables.

Registry No. **1a**, 91410-27-4; **1b**, 111349-24-7; **1c**, 137466-31-0; **1d**, 94249-91-9; **1e**, 137466-32-1; **2a**, 137466-22-9; **2b**, 137466-24-1; **2c**, 137466-26-3; **2d**, 137466-28-5; **2e**, 137466-30-9; **2f**, 137494-31-6; **3**, 137466-34-3; **4**, 137466-36-5; **5a**, 137494-33-8; **5b**, 137466-38-7; **5c**, 137494-35-0; **5d**, 137466-40-1; **5e**, 137466-42-3; **5e-d**, 137466-50-3; **5f**, 137494-37-2; **6a**, 137466-44-5; **6b**, 137494-39-4; **6c**, 137466-46-7; **6f**, 137466-48-9; diphpyH$_2$, 3558-69-8; ditolpyH$_2$, 14435-88-2.

Supplementary Material Available: Tables of positional parameters and temperature factors, including the H atoms, full distances and bond angles, torsion or conformation angles, and anisotropic temperature factors (14 pages); a listing of structure factors (40 pages). Ordering information is given on any current masthead page.

Reactions of [Cp*Ru(OMe)]$_2$. 9.[1] Olefin Activation and Formation of Allyl Complexes. Molecular Structure of Cp*Ru(η^3-C$_3$H$_5$)(η^2-CH$_2$=CHCH$_3$)

U. Koelle,* Byung-Sun Kang, T. P. Spaniol, and U. Englert

Institute of Inorganic Chemistry, Technical University of Aachen, Prof.-Pirlet.-Strasse 1, W-5100 Aachen, FRG

Received April 24, 1991

Simple olefin addition products of [Cp*Ru(OMe)]$_2$ (1) are unstable at ambient temperature. Under slightly more forcing conditions the allyl complexes Cp*Ru(C$_3$H$_4$Me)(C$_2$H$_4$) (3) and Cp*Ru(C$_3$H$_5$)(C$_2$H$_3$Me) (4) are formed with ethylene and propylene, respectively. 4 crystallizes in the space group *Pbca* with a = 13.752 (3) Å, b = 14.576 (2) Å, c = 15.174 (4) Å, and Z = 8; R (R_w) = 0.027 (0.035) for 1837 independent reflections with $I > 3\sigma(I)$. Reaction of 1 with cyclic polyolefins proceeds with hydrogenation or dehydrogenation of the ligand to give Cp*Ru(π-olefin) complexes.

Activation of olefins for oligomerization and polymerization at transition-metal centers still offers much attraction. Generally a labile precursor complex is treated with the olefin, upon which this latter species enters into vacancies of the coordination sphere generated by thermally or photochemically induced dissociation of some ligand.

The coordinatively unsaturated Ru complex [Cp*Ru(OMe)]$_2$ (1),[2-4] in contrast, has been shown to directly add common σ-donor–π-acceptor ligands such as PR$_3$, bpy, and CO[2,3] with and without cleavage of the dimer, depending on the conditions. The dimer itself offers two vacant coordination sites, and a further ligand may be added to each Ru on cleavage. This bonding situation offers many of the features commonly considered as prerequisites for a catalytically active metal center.

In the following contribution, we described addition and coupling reactions of ethylene, propylene, cyclohexadiene, and cyclooctatetraene with 1.

Results

Reaction of 1 with Ethylene and Propylene. Coordination of olefins to 1, despite the coordinatively unsaturated character of the methoxo complex, does not result in addition of simple mono- or diolefins to give isolable olefin alkoxo complexes under ambient conditions. Chelating 1,5-cyclooctadiene reacts with 1 at ambient temperature in the presence of LiCl by exchange of OMe for Cl and formation of Cp*Ru(COD)Cl[5] or, under hexane reflux over 12 h, with elimination of formaldehyde and formation of the hydride Cp*Ru(COD)H.[6] To further elucidate possible activation of olefins by 1, we have investigated its reaction with ethylene, propylene, and cycloolefins.

When the cherry red solution of 1 in MeOH is saturated at −50 °C with ethylene, the adduct 2 separates as a light yellow precipitate. The color change, characteristic of

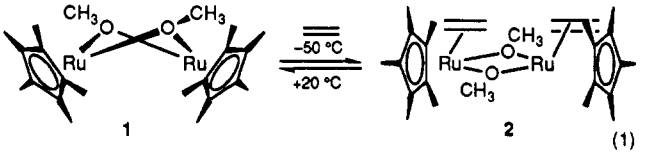

1 2 (1)

adduct formation, has been observed with other π-acceptor ligands, e.g. phosphines.[2] However, adduct 2 is readily dissociated into its constituents at room temperature in solution or as a solid. Attempted isolation of the low-temperature compound gave, after warming to room tem-

(1) Part 6: Koelle, U.; Wang, M. H.; Raabe, G. *Organometallics* **1991**, *10*, 2573.
(2) (a) Koelle, U.; Kossakowski, J. *J. Chem. Soc., Chem. Commun.* **1988**, 549. (b) Koelle, U.; Kossakowski, J. *J. Organomet. Chem.* **1989**, *362*, 383.
(3) Koelle, U.; Kossakowski, J. *Inorg. Synth.*, in press.
(4) Loren, S. D.; Campion, B. K.; Heyn, R. H.; Don Tilley, T.; Bursten, B. E.; Luth, K. W. *J. Am. Chem. Soc.* **1989**, *111*, 4712.
(5) Koelle, U.; Kang, B.-S.; Raabe, G.; Krüger, C. *J. Organomet. Chem.* **1990**, *386*, 261.
(6) Koelle, U.; Kang, B.-S.; Thewalt, U. *J. Organomet. Chem.* **1990**, *386*, 267.

0276-7333/92/2311-0249$03.00/0